

Predicting nuclear masses with product-unit networks

Babette Dellen¹, Uwe Jaekel¹, Paulo S. A. Freitas², and John W. Clark^{2,3}

¹University of Applied Sciences Koblenz, 53424 Remagen, Germany

²University of Madeira, Campus Universitário da Penteada, 9020-105 Funchal, Portugal

³Washington University in St. Louis, St. Louis, MO 63130, USA

Abstract

Accurate estimation of nuclear masses and their prediction beyond the experimentally explored domains of the nuclear landscape are crucial to an understanding of the fundamental origin of nuclear properties and to many applications of nuclear science, most notably in quantifying the r -process of stellar nucleosynthesis. Neural networks have been applied with some success to the prediction of nuclear masses, but they are known to have shortcomings in application to extrapolation tasks. In this work, we propose and explore a novel type of neural network for mass prediction in which the usual neuron-like processing units are replaced by complex-valued product units that permit multiplicative couplings of inputs to be learned from the input data. This generalized network model is tested on both interpolation and extrapolation data sets drawn from the Atomic Mass Evaluation. Its performance is compared with that of several neural-network architectures, substantiating its suitability for nuclear mass prediction. Additionally, a prediction-uncertainty measure for such complex-valued networks is proposed that serves to identify regions of expected low prediction error.

1 Introduction

The mass of a nucleus (Z, N), specified by its respective proton and neutron contents, is arguably its most fundamental experimentally derived property, because the difference from the sum of its proton and neutron rest masses determines its binding energy due to interactions between these constituents. Often this difference is referred to as the mass defect. Its accurate measurement and theoretical prediction are central to a deep understanding of the origin of the elements as well as fundamental nuclear interactions, and

ultimately important for many applications of nuclear science [19, 14].

With respect to theoretical prediction, diverse mass formulas as a function of Z and N have been proposed or derived, beginning with the phenomenological macroscopic liquid-drop model [8, 24], followed in time by related semi-empirical macroscopic-microscopic models such as the sequences of Finite-Range Droplet Models (FRDM) and Weizsäcker-Skyrme (WS) Models that incorporate specific quantum phenomena such as shell structure and nucleonic pairing. For information on recent developments in this category, see especially Refs. [26, 20, 17, 27].

The third traditional category of mass models rests on fundamental theory and hence is microscopic, in the sense the models are based on assumed nucleon-nucleon interactions. However, the corresponding Schrödinger equation for the many-nucleon problem becomes intractable with increasing $A = N + Z$ and approximations are necessary. Typical approaches in this category are based on density functionals and involve assumed nucleon-nucleon interactions that allow mean-field treatments (see, for example, Ref. [11]). True microscopic quantum many-body calculation of nuclear masses, notably by quantum Monte Carlo techniques, soon becomes intractable with increasing A due to combinatoric explosion. Developments in quantum computation show promise of overcoming this barrier [4].

An important goal of mass models is to achieve an accuracy level of predictions below a root mean squared (RMS) error of 0.100 MeV, in order to be useful for research on the r -process, which is responsible for the creation of about half of the nuclei heavier than iron. Among the traditional methods indicated above, the best performance in this respect may be represented by the WS4 model in the Weizsäcker-Skyrme series, still well short of the target.

Machine learning (ML) techniques provide a quite different approach to the prediction of nuclear properties that has gained wide acceptance in the last decade and seen rapid growth of applications in diverse variants [3]. Such methods have the advantage that, beyond the raw data, only minimal additional knowledge of the relevant laws of physics is required for their implementation. Multilayer neural networks have served as a prime example, with successful applications to nuclear masses and other properties beginning in the early 1990s [9, 10, 2, 1]. For recent applications of neural networks and related ML techniques for prediction of nuclear masses, see especially Refs. [23, 18, 16, 22, 21].

Feedforward neural networks with at least one hidden layer have been of particular interest because they have been proven to be universal function approximators [5] that can adapt to any kind of data. However, a successful predictive model may involve a large number of adjustable parameters that must be estimated by optimization. A recently proposed neural network for mass prediction achieved RMS errors below 0.4 MeV on training data, but required the fitting of close to a million model parameters [16]. In contrast, Lovell et al. [18] developed a probabilistic neural network for mass prediction that incorporated theoretical knowledge by providing components of phenomenological models as input features. With this strategy the number of neurons in the network (and hence the number of parameters) could be reduced significantly, while achieving mass prediction with RMS errors in the range 0.56 – 3.9 MeV. (It must be noted, however, that RMS errors reported for different mass studies depend crucially on the choices of data sets and input features and accordingly must be interpreted and compared with caution.)

Beyond describing available data with high accuracy using the previously mentioned approaches, there is a critical need for reliable extrapolation to lesser known regions of the nuclear chart. While a particular model may perform very well on the data set that was used for determining the model parameters, its performance is, in general, likely to fall off beyond this domain. For example, traditional neural networks have been shown to perform poorly in extrapolation tasks [12, 6]. In part, this can be understood as a consequence of thresholding: Thresholds and threshold-like activation functions used in neural networks compartmentalize the feature space and provide,

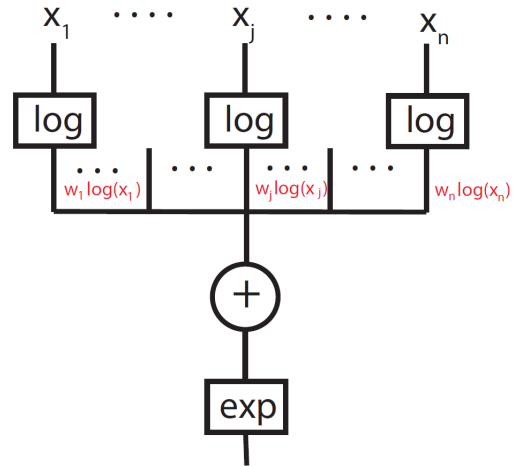


Figure 1: Product unit using the logarithmic and exponential function as activations to implement multiplicative couplings [6]. In the complex case, $w_j \in \mathbb{C}$ and $x_j \in \mathbb{C} \setminus \{0\}$ for $j = 1, \dots, n$.

in some simplification, a piece-wise linear approximation of the input-output relationship which impairs the extrapolation capabilities of the network.

A recent study indicates that product-unit networks are superior to standard feedforward neural networks in function and pattern extrapolation tasks [6]. Such networks are composed of nonlinear processing units that enable representation of multiplicative couplings of inputs [7, 15, 6] (see Fig. 1). Since the information capacity of each nonlinear unit is expected to be larger than that of ordinary linear units, product-unit networks require fewer neuronal units than classical neural networks in modeling the same function. Moreover, the trained weights of the product units provide useful information about correlations between input features, potentially furnishing insight into the physical laws underlying the measured data and contributing to model discovery.

These special advantages motivated us to adapt and further develop product-unit networks for the prediction of nuclear masses and to evaluate their performance in both interpolation and extrapolation tasks. In doing so, we were led quite naturally to propose a novel complex-valued product-unit network that does not require thresholds or threshold-like activations, thereby further improving performance in extrapolation, their elimination being an advantage in itself as indicated above. Therefore we compare the proposed complex-valued product-unit network to several alternative real-valued product-unit networks operating with thresholds and classical multilayer

perceptrons. A further novelty of this generalization is that the introduction of a prediction-uncertainty measure derived from the imaginary spill of the complex-valued network output allows one to identify low-error predictions beyond the experimentally explored domain.

2 Methods

2.1 Real-valued product-unit networks

Product units compute the products of inputs x_j , where $j = 1, \dots, n$, raised to the power of their weights w_j , yielding $\prod_j x_j^{w_j}$. They can in fact be implemented with conventional neural networks by using both logarithmic and exponential functions as activations, as shown in Fig. 1 [6]. For example, the product a^2b can be represented as $\exp(2 \log a + \log b)$. By combining product units in parallel and summing their weighted outputs, input-output relationships of the type $\sum_k \alpha_k \prod_j x_j^{w_{jk}}$ can be described [6]. Such networks can be trained using gradient descent and other standard optimization methods. A disadvantage of real-valued product units is that they are not defined for non-positive inputs. However, if the input is directly passed to a layer composed of product units, this constraint can be addressed by appropriately shifting the input values. If real-valued product units are being incorporated into larger network structures, thresholds have to be applied that allow only positive data to pass.

The architectures of various real-valued networks used in this work are summarized in Table 1. The network RPUN consists of 50 product units followed by a single linear output unit. No thresholds are applied. This network is defined only for positive inputs. The networks HPUN-S and HPUN-L are hybrid networks that are composed of a linear layer with ReLU-activation, i.e., $f(x) = \max(\epsilon, x)$, where ϵ is a very small number, followed by a product-unit layer and a single linear output neuron. This network structure allows transformations of the input data to be learned as well. The ReLU-activation ensures that only positive outputs are passed to the next layer.

For comparative purposes during evaluation, we also investigated two classical multilayer perceptrons with ReLU activation. The network MLP-L contains two hidden layers and the network MLP-XL has three.

To optimize the real-valued networks, we use squared differences as loss function. For the RPUN network (implemented in Matlab) opti-

mization was performed using stochastic gradient descent and training until convergence for 20,000 epochs. For the hybrid networks and the multilayer perceptron (implemented in Pytorch), Adam-optimization (including a learning-rate scheduler) with a batch size of 500 was used. We trained until convergence for 50,000 epochs. Results may vary pending on initialization and hyperparameter choices.

2.2 Complex-valued product-unit networks

Another and indeed more elegant way to handle non-positive data is to introduce complex-valued product-unit networks, i.e., networks with complex-valued weights and complex activations. To enable linear transformations of the input data, a linear complex-valued preprocessing layer is added to the network. In complex space, the logarithmic function is also defined for negative inputs. However, the non-zero constraint still applies. Interestingly, this rarely poses a problem, because in complex space, weights do not have to cross the origin to change the sign of their real part during optimization. Application of complex-valued product-unit networks thus allows one to incorporate processing units without having to include thresholds. Here we investigate complex-valued product-unit networks of three different sizes, named CPUN-L, CPUN-S, and CPUN-XS (see Table 1). Their output is a complex number $z = x + iy$. To optimize the network, we therefore use $(x - \hat{x})^2 + y^2$ as loss function, where \hat{x} is the real-valued experimentally measured mass defect of the nucleus. These networks are implemented in Pytorch with Adam-optimization using a batch size of 500 and a learning-rate scheduler. The real part of the output is used to represent nuclear mass. Results may vary pending on initialization and hyperparameter choices.

In experiment B, we trained for an additional 10,000 epochs to average the RMS errors and the prediction uncertainties over this additional training period. In doing so, small random effects induced by the batch size which are more likely to occur in product-unit networks could be removed.

2.3 Data sets

The atomic mass evaluation AME2020 provides atomic mass values together with their measurement uncertainties [13, 25]. This data collection was used to generate a training data set Train-

Table 1: Specifications of various networks built from product units (PU), linear units (LU) and ReLU activations (ReLU). CPUN-XS, CPUN-S and CPUN-L are complex-valued product unit networks of different sizes.

Layer	RPUN	CPUN-XS	CPUN-S	CPUN-L	HPUN-S	HPUN-L	MLP-L	MLP-XL
Input	2	10	10	10	10	10	10	10
Hidden 1	50 PU	10 LU	10 LU	20 LU	10 LU + ReLU	20 LU + ReLU	20 LU + ReLU	40 LU + ReLU
Hidden 2	x	10 PU	20 PU	40 PU	20 PU	40 PU	40 LU + ReLU	40 LU + ReLU
Hidden 3	x	x	x	x	x	x	x	40 LU + ReLU
Output	1 LU	1 LU	1 LU	1 LU	1 LU	1 LU	1 LU	1 LU

A composed of 2827 nuclei and an interpolation test set Inter-A composed of randomly selected 730 nuclei (roughly 25%). These data were used in *Experiment A*.

In *Experiment B*, we explored the extrapolation capabilities of the networks of Table 1. Here we used, in addition, an earlier data set, namely FRDM2012 [20], in providing experimentally established nuclear masses. From this resource, 2149 data points were split into a training set train-B containing 2099 data points and an interpolation test set Inter-B composed of 50 randomly selected nuclei. Also selected is an extrapolation test set Extra-B composed of nuclei of the AME2020 data set that have a mass uncertainty value smaller than 0.5 MeV and are not part of Train-B. The test set Extra-B contains 1022 data points. So as not to impair extrapolation performance by reducing the size of the training set, Inter-B contains only a small amount of data.

For comparative evaluation, we generated in Experiment C another pair of training and test sets by splitting the data set Train-B randomly into two sets. Train-C contains 1949 nuclei and Inter-C, 200. Similarly, 336 nuclei were selected from AME2020 to generate the extrapolation test set Extra-C1. Only nuclei with a mass uncertainty smaller than 0.17 MeV entered the latter data set, while limiting the range of N and Z values. This was done to obtain data sets similar to those used in [16]. We also generated a second extrapolation test set to include nuclei with larger N and Z , resulting in the set Extra-C2 containing 44 nuclei. The color-coded map of the data sets involved in Experiment C is shown in Fig. 5d.

Table 2: Experiment A: Standard deviation (RMS error) in MeV (rounded) for the data sets Train-A and Inter-A, as obtained with the RPUN and CPUN-L networks.

Network	σ_{TrainA}	σ_{InterA}
RPUN	2.86	2.87
CPUN-L	0.51	0.78

3 Results

3.1 Experiment A: Input features and multiplicative couplings

Here we first investigated a real-valued product-unit network of 50 product units that has as input variables only the proton and neutron numbers Z and N (network RPUN), a very basic exemplar. Using stochastic gradient descent, convergence was achieved after 20,000 epochs. The standard deviation was computed for the training and test sets, i.e., Train-A and Inter-A, as shown in Table 2. The standard deviations (RMS errors) for the training and interpolation test data are in the same range, indicating little or no overfitting. Even though the RMS error is still large, this network outperforms the probabilistic neural network M2 of Ref. [18], in which an RMS error of 3.9 MeV was reported for a training set of 2074 nuclei from the 2016 Atomic Mass Evaluation (AME2016). However, these results cannot be directly compared, since we use a larger training set of 2827 nuclei that also contains mass values afflicted with large uncertainty.

In Fig. 2, the exponents of the product units are shown for Z and N . Exponents of product

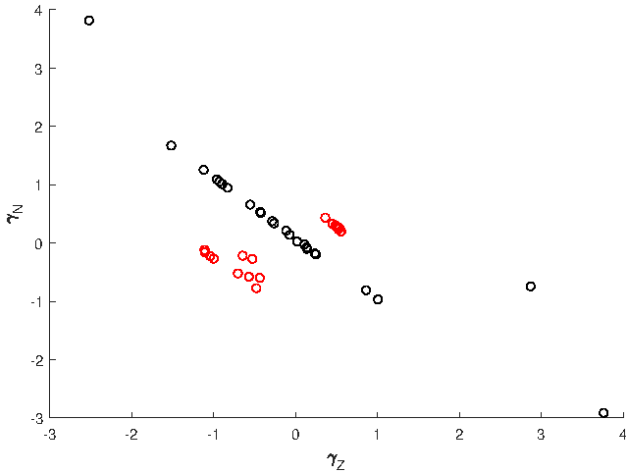


Figure 2: Experiment A: Exponents of the product units of the real-valued product-unit network RPUN are shown in exponent space. The network RPUN revealed in some approximation a functional dependence of the mass excess on Z and N of the form $f(Z/N)g(N)$, where f and g are functions.

units with a negative weight factor are shown as red circles; those with positive ones as black circles. The size of the circles increases with increasing weight factor. Some circles are coincident due to product units having the same exponents. A regular structure is revealed that suggests a functional dependency of the mass excess on Z and N of the form $f(Z/N)g(N)$, where f and g are functions. The heat map for the differences between predicted and true mass values as a function of Z and N (as seen in Fig. 3a and 3b) shows large errors in the vicinity of magic numbers. Fine repetitive errors indicate a dependence of mass on parity.

To improve the model, information about the proximity to the magic numbers was included with the input data. Accordingly, we added two features to the input data, namely the distance to the closest magic number of Z and the distance to closest the magic number of N , for a number of nuclei. For protons, the magic numbers 2, 8, 20, 28, 50, 82, 126, 164 were included, and for neutrons neutrons, 2, 8, 20, 28, 50, 82, 126, 184, 196. For each data point, we computed first the distance from the closest magic numbers, separately for protons and neutrons. Additionally, we included features indicating odd and even parities for N , Z , and A . By training the network CPUN-L with this extended set of input features, ten in number, the predictions could be improved (see Table 2). As a result,

Table 3: Experiment B: RMS error in MeV (rounded) for the CPUN-L network for different thresholds τ .

Data set	τ	N	σ
Extra-B	-	1022	4.12
Extra-B	5	959	1.85
Extra-B	0.1	256	0.55
Extra-B	0.04	30	0.39
Inter-B	-	50	0.36
Inter-B	0.1	44	0.18
Train-B	—	2099	0.15

a training RMS error of 0.51 MeV was achieved.

The absolute mass difference is shown in Fig. 3c. Compared to the model RPUN, the error in the vicinity of the magic numbers has decreased, as has that associated with parity effects. Larger errors above 1 MeV are more frequently observed for small atomic numbers. This may indicate that the input features selected are not carrying sufficient information to model the data more accurately in that region.

3.2 Experiment B: Mass extrapolation and prediction uncertainty

We have investigated the extrapolation capability of the complex-valued product-unit network CPUN-L, trained with the data set Train-B, containing 2099 nuclei. Unlike the data set used in Experiment A, the training data now includes only nuclei with well-established mass values of low uncertainty. After 60,000 epochs, an RMS error of 0.15 is achieved for the training set (see Table 3), outperforming recent approaches evaluated on similar data [18, 16]. In particular, Ref. [16] reported a training error of 0.263 MeV for a similar data set by predicting the residual between the liquid-drop-model prediction and the true mass, using a deep neural network containing over a million parameters. In contrast, an RMS error of 0.56 MeV has been achieved far more economically with a probabilistic neural network [18].

Since performance evaluation on training data has limited significance for performance on other data, we have evaluated model performance further on a large extrapolation test set containing 1022 nuclei partially afflicted with large uncertainty, but below 0.5 MeV. We also evaluated interpolation performance using a small interpolation test set containing 50 nuclei. As expected, the

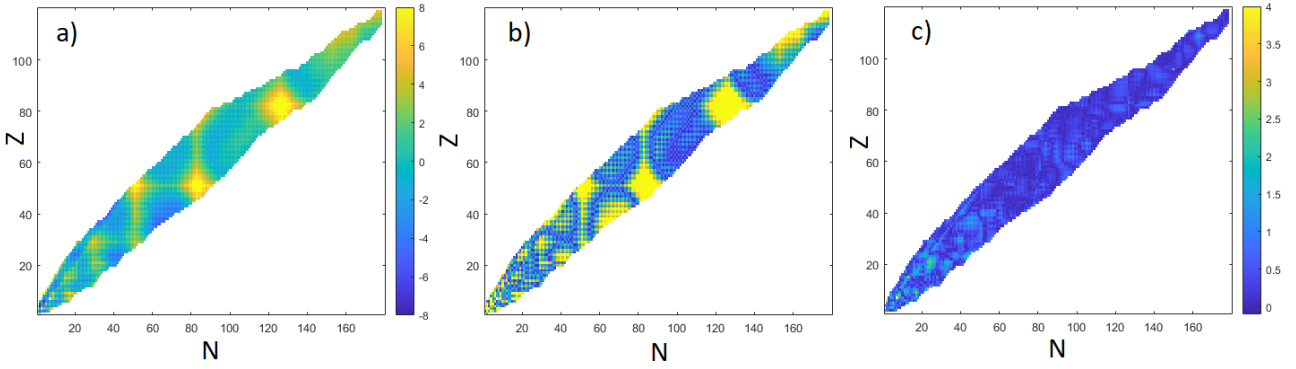


Figure 3: Experiment A: (a-b) Differences between predicted mass and true mass in MeV show larger errors in the vicinity of magic numbers. The finer patterns in the differences repeat with respect to parity. (c) Including additional features (magic numbers, parity) and using the CPUN-L model improves predictions. Larger differences are observed for small atomic numbers.

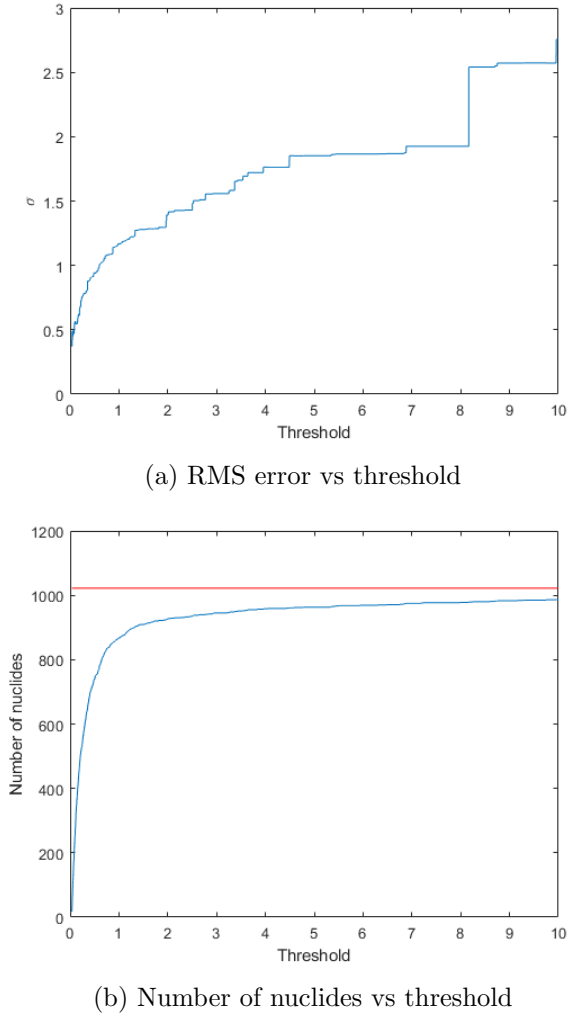


Figure 4: Experiment B: (a) RMS error in MeV plotted as a function of threshold τ . (b) Size of data sets in number of nuclei, plotted as a function of τ .

RMS error is larger for the test data. An RMS error of 4.12 MeV was obtained for the large extrapolation data set, and an RMS error of 0.36 MeV for the interpolation test set.

Importantly, however, we can identify subsets of test data with a lower RMS error by using the imaginary component of the output to measure prediction uncertainty. In Figure 5a, the absolute mass differences between predicted and true values are shown for the extrapolation set. Fig. 5b shows the absolute value of the imaginary component of the output, defining the prediction uncertainty. It provides a useful indicator for erroneous predictions.

By applying a threshold τ to the prediction uncertainty, we can select subsets of nuclei and calculate the RMS error for a chosen subset. In Figure 4a the RMS error is plotted as a function of τ , and seen to decrease with τ . The size of the subsets decreases as well, as shown in Figure 4b. A similar behavior is observed for the interpolation set (not shown). The results for a set of thresholds are summarized in Table 3. For the interpolation test set, it is possible to predict masses that have not been included in the training set with an RMS error below 0.2 MeV. For extrapolation, the RMS error for mass prediction could be reduced to 0.39 MeV.

3.3 Experiment C: Performance evaluation and comparison

This experimental sequence is devoted to further comparison of the performance of the network CPUN-L and the other network architectures specified in Table 1. The extrapolation data set used for Experiment B contains many nu-

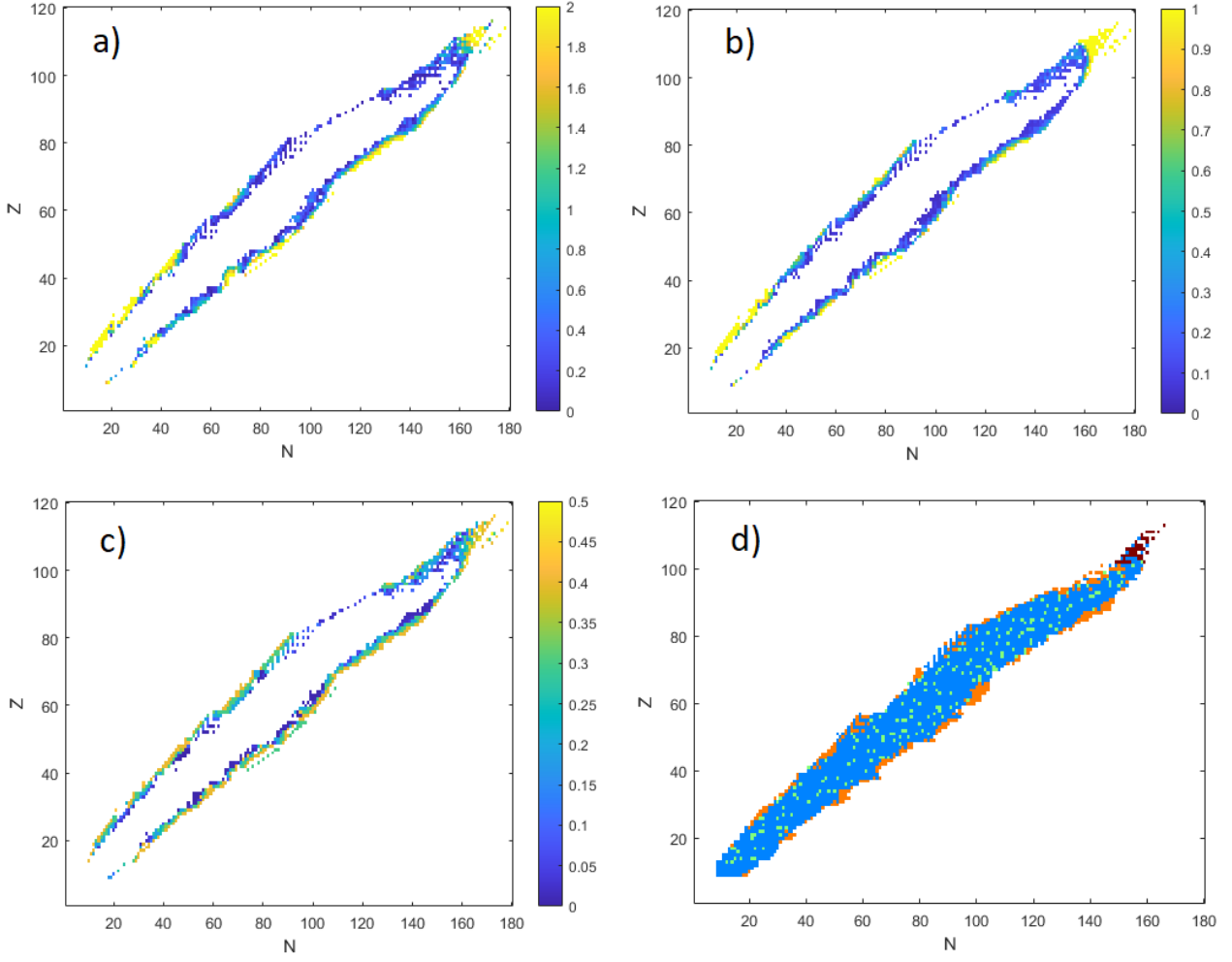


Figure 5: (a) Absolute difference between predicted and true masses in MeV in Experiment B. (b) Absolute value of the imaginary part of the output of CPUN-L provides a prediction uncertainty for predicted masses in Experiment B. (c) Heat map of measurement uncertainties (AME2020) in MeV for the masses in the extrapolation region. (d) Training and test sets used in Experiment C: Train-C (blue), Inter-C (light blue), Extra-C1 (orange), Extra-C2 (dark red).

Table 4: Experiment C: RMS error in MeV (rounded) for the training and test sets, for different networks.

Data	CPUN-XS	CPUN-S	CPUN-L	HPUN-S	HPUN-L	MLP-L	MLP-XL
Train-C	0.54	0.37	0.17	0.56	0.38	0.77	0.37
Inter-C	0.49	0.38	0.26	0.60	0.45	0.90	0.51
Extra-C1	0.73	0.66	0.39	1.55	0.98	1.58	1.23
Extra-C2	1.23	0.74	0.65	2.72	1.13	1.79	3.53

clei measured with a large mass uncertainty (see Fig. 5c). By keeping only nuclei with mass uncertainty smaller than 0.17 MeV, an extrapolation data set presumably similar to that used in Ref. [16] could be assembled (see orange-colored nuclei in Figure 5d). We also evaluated relative performance for an additional extrapolation set containing nuclei with large atomic masses (nuclei colored dark red). The interpolation test data is shown in light blue, the training data in darker blue.

The results after 50,000 epochs are shown in Table 4 for the different networks listed. The network CPUN-L outperforms the other networks on all data sets, achieving an RMS error of 0.17 MeV for the training set, 0.39 MeV for the extrapolation test set Extra-C1, and 0.65 MeV for the extrapolation test set Extra-C2. The deep multilayer perceptron MLP-XL achieved a training and interpolation error in the range of most product-unit networks (except CPUN-L), but is less suited to predict nuclear masses at larger distance from the training set than the product-unit networks. We suspect that the use of thresholds (ReLU activations) impairs the extrapolation capabilities of the MLP.

The network CPUN-L also outperforms a recent deep-learning model [16] in the extrapolation task. Ref. [16] obtained an RMS error of 0.263 MeV for the training set and 0.605 MeV for an extrapolation set that we presume to be approximately identical with data set Extra-C1.

4 Conclusion

We have proposed a novel type of neural network for nuclear-mass prediction. The model is composed of product units that allow multiplicative couplings of inputs to be learned from the data. This mechanism enables the capture of hidden structures that are not accessible by classical neural networks. By working with complex-valued weights and activations, we could propose a product-unit network (CPUN-L) that delivers predictions with an RMS error well below 0.2 MeV in the experimentally explored domain of the nuclear chart, as well as for a group of selected nuclei within a random test set. We have further identified groups of nuclei in the extrapolation region with an RMS error below 0.4 MeV. Regions of low-error predictions were identified using a novel prediction-uncertainty measure that is specific for this type of network.

We have compared a variety of network structures and shown that the complex-valued network CPUN-L performs best in terms of training RMS error and both interpolation and extrapolation test-set RMS errors. The networks used in this study have been small compared with deep networks currently employed for similar tasks [16]. It is certainly possible to further improve training performance by adding more layers and neurons (thus parameters) to the networks studied here, including the classical multilayer perceptron, but only at the risk of serious overfitting, i.e., an increase of the RMS error for the test data, especially the extrapolation test set.

References

- [1] S. Athanassopoulos, E. Mavrommatis, K. Gernoth, and J. W. Clark. Nuclear mass systematics by complementing the finite range droplet model with neural networks. *HNPS Proceedings*, 14, 12 2005.
- [2] S. Athanassopoulos, E. Mavrommatis, K. A. Gernoth, and J. W. Clark. Nuclear mass systematics using neural networks. *Nuclear Physics A*, 743(4):222–235, 2004.
- [3] A. Boehnlein, M. Diefenthaler, N. Sato, M. Schram, V. Ziegler, C. Fanelli, M. Hjorth-Jensen, T. Horn, M. P. Kuchera, D. Lee, W. Nazarewicz, P. Ostroumov, K. Orginos, A. Poon, X.-N. Wang, A. Scheinker, M. S. Smith, and L.-G. Pang. Colloquium: Machine learning in nuclear physics. *Rev. Mod. Phys.*, 94:031003, Sep 2022.
- [4] J. Carlson, D. J. Dean, M. Hjorth-Jensen, D. Kaplan, J. Preskill, K. Roche, M. J. Savage, and M. Troyer. Quantum computing for theoretical nuclear physics, a white paper prepared for the u.s. department of energy, office of science, office of nuclear physics. 1 2018.
- [5] G. Cybenko. Approximations by superpositions of sigmoidal functions. *Mathematics of Control, Signals, and Systems*, 2:303 – 314, 4 1989.
- [6] B. Dellen, U. Jaekel, and M. Wolnitza. Function and pattern extrapolation with product-unit networks. In J. M. F. Rodrigues et al., editors, *Computational Science – ICCS 2019*, pages 174–188. Springer International Publishing, 2019.

- [7] R. Durbin and D. E. Rumelhart. Product units: A computationally powerful and biologically plausible extension to backpropagation networks. *Neural Computation*, 1(1):133–142, 1989.
- [8] G. Gamow. Mass defect curve and nuclear constitution. *Proc. R. Soc. Lond. A*, 126:632–644, 1930.
- [9] S. Gazula, J. W. Clark, and H. Bohr. Learning and prediction of nuclear stability by neural networks. *Nuclear Physics A*, 540(1):1–26, 1992.
- [10] K. A. Gernoth, J. W. Clark, J. S. Prater, and H. Bohr. Neural network models of nuclear systematics. *Physics Letters B*, 300(1):1–7, 1993.
- [11] S. Goriely, N. Chamel, and J. M. Pearson. Further explorations of skyrme-hartree-fock-bogoliubov mass formulas. xvi. inclusion of self-energy effects in pairing. *Phys. Rev. C*, 93:034337, Mar 2016.
- [12] P. Haley and D. Soloway. Extrapolation limitations of multilayer feedforward neural networks. In *IJCNN International Joint Conference on Neural Networks*, pages 25 – 30 vol.4, 07 1992.
- [13] W. Huang, M. Wang, F. Kondev, G. Audi, and S. Naimi. The ame 2020 atomic mass evaluation (i). evaluation of input data, and adjustment procedures*. *Chinese Physics C*, 45(3):030002, mar 2021.
- [14] T. Kawano, S. Chiba, and H. Koura. Phenomenological nuclear level densities using the ktuy05 nuclear mass formula for applications off-stability. *Journal of Nuclear Science and Technology - J NUCL SCI TECHNOL*, 43:1–8, 01 2006.
- [15] L. R. Leerink, C. L. Giles, B. G. Horne, and M. A. Jabri. Learning with product units. *Advances in Neural Information Processing Systems*, 7:537, 1995.
- [16] C.-Q. Li, C.-N. Tong, H.-J. Du, and L. Pang. Deep learning approach to nuclear masses and α -decay half-lives. *Physical Review C*, 2022.
- [17] M. Liu, N. Wang, Y. Deng, and X. Wu. Further improvements on a global nuclear mass model. *Phys. Rev. C*, 84:014333, Jul 2011.
- [18] A. E. Lovell, A. T. Mohan, T. M. Sprouse, and M. R. Mumpower. Nuclear masses learned from a probabilistic neural network. *Phys. Rev. C*, 106:014305, Jul 2022.
- [19] M. R. Mumpower, R. Surman, G. C. McLaughlin, and A. Aprahamian. The impact of individual nuclear properties on r-process nucleosynthesis. *Progress in Particle and Nuclear Physics*, 86:86–126, jan 2016.
- [20] P. Möller, A. J. Sierk, T. Ichikawa, and H. Sagawa. Nuclear ground-state masses and deformations: FRDM(2012). *Atomic Data and Nuclear Data Tables*, 109-110:1–204, may 2016.
- [21] L. Neufcourt, Y. Cao, S. A. Giuliani, W. Nazarewicz, E. Olsen, and O. B. Tarasov. Quantified limits of the nuclear landscape. *Phys. Rev. C*, 101:044307, Apr 2020.
- [22] L. Neufcourt, Y. Cao, W. Nazarewicz, and F. Viens. Bayesian approach to model-based extrapolation of nuclear observables. *Phys. Rev. C*, 98:034318, Sep 2018.
- [23] Z. M. Niu, J. Y. Fang, and Y. F. Niu. Comparative study of radial basis function and bayesian neural network approaches in nuclear mass predictions. *Phys. Rev. C*, 100:054311, Nov 2019.
- [24] C. F. von Weizsäcker. Zur theorie der kernmassen. *Zeitschrift für Physik*, 96:431–458, 1935.
- [25] M. Wang, W. Huang, F. Kondev, G. Audi, and S. Naimi. The ame 2020 atomic mass evaluation (ii). tables, graphs and references*. *Chinese Physics C*, 45(3):030003, mar 2021.
- [26] N. Wang, M. Liu, X. Wu, and J. Meng. Surface diffuseness correction in global mass formula. *Physics Letters B*, 734:215–219, jun 2014.
- [27] H. Zhang, J. Dong, N. Ma, G. Royer, J. Li, and H. Zhang. An improved nuclear mass formula with a unified prescription for the shell and pairing corrections. *Nuclear Physics A*, 929:38–53, 2014.